

The molecular dynamics calculations were done by using the MOLSIM system. Figures 5-7 and 10 were made by using the MicroChem molecular modeling software.

Registry No. sPS, 28325-75-9.

## References and Notes

- (1) Hopfinger, A. J. *Conformational Properties of Macromolecules*; Academic Press: New York, 1973.
- (2) Orchard, B. J.; Tripathy, S. K.; Pearlstein, R. A.; Hopfinger, A. J. *J. Comput. Chem.* **1987**, *8*, 28.
- (3) Ishihara, N.; Seimiya, T.; Kuramoto, M.; Ubi, M. *Macromolecules* **1986**, *19*, 2464.
- (4) Chatani, Y.; Fujii, Y.; Shimane, Y.; Ijitsu, T. *Polym. Prepr. Jpn.* **1988**, *37*, 26-0-12.
- (5) Kobayashi, M.; Nakaoki, T.; Uoi, M. *Polym. Prepr. Jpn.* **1988**, *37*, 26-0-20.
- (6) Corradini, P.; Natta, G.; Ganis, P.; Temussi, P. A. *J. Polym. Sci. Part C* **1967**, *16*, 2477.
- (7) (a) Natta, G.; Peraldo, M.; Allegra, G. *Makromol. Chem.* **1966**, *9*, 181. (b) Tadokoro, H.; Kobayashi, M.; Kobayashi, S.; Yasufuku, K.; Mori, K. *Rep. Prog. Polym. Phys. Jpn.* **1966**, *9*, 181.
- (8) Hopfinger, A. J. *J. Med. Chem.* **1985**, *28*, 1133.
- (9) Yoon, D. Y.; Sundarajan, P. R.; Flory, P. J. *Macromolecules* **1975**, *8*, 776.
- (10) Natta, G.; Corradini, P.; Bassi, I. W. *Nuovo Cimento, Suppl.* **1960**, *15*, 68.
- (11) Pople, J. A.; Santry, D. P.; Segal, G. A. *J. Chem. Phys.* **1965**, *43*, 5129. Pople, J. A.; Segal, G. A. *Ibid.* **1965**, *43*, 5136; **1966**, *44*, 3289.
- (12) Pearlstein, R. A. *CHEMLAB-II Users Guide*; Chemlab: 1780 Wilson Dr., Lake Forest, IL 60045, Jan 1988.
- (13) Allinger, N. L.; Yuh, Y. H. Operating Instructions for MM2 and MMP2 Program—1977 Force Field. *QPCE* **1980**.
- (14) McCammon, J. A.; Harvey, S. *Dynamics of Proteins and Nucleic Acids*; Cambridge University Press: London, 1987.
- (15) Girolamo, M.; Keller, A.; Miyasaka, K.; Overbergh, N. *J. Polym. Sci., Polym. Phys. Ed.* **1976**, *14*, 39.
- (16) Atkins, E. D. T.; Isaac, D. H.; Keller, A.; Miyasaka, A. *J. Polym. Sci., Polym. Phys. Ed.* **1977**, *15*, 211.
- (17) Tadokoro, H. *Structure of Crystalline Polymers*; Wiley-Interscience: New York, 1979.
- (18) Natta, G.; Corradini, P. *J. Polym. Sci.* **1956**, *20*, 251.

## An Off-Lattice Constant-Pressure Simulation of Liquid Polymethylene

Richard H. Boyd

Department of Materials Science and Engineering and Department of Chemical Engineering, University of Utah, Salt Lake City, Utah 84112. Received September 12, 1988

**ABSTRACT:** An off-lattice constant-pressure Monte Carlo simulation has been carried out for a model of liquid polymethylene. Reptation was used as the Monte Carlo move. Methylene units were represented by united atom beads with nonbonded potentials of interaction between them. Intramolecular torsional potentials were used, but the molecules were rigid with respect to bond stretching and bending. The system consisted of 32 chains of 24 methylene units each. PVT data were generated over the ranges 300–500 K and 1–1000 atm. The equilibrium volume at 1 atm is in good agreement (2%) with that for tetracosane. The thermal expansion at 1 atm and the isothermal compressibility at 450 K agree well with experiment for polyethylene. Harmonic vibrational analysis was carried out separately for representative configurations of the molecules in the system and the resulting calculated vibrational heat capacity added to the intermolecular heat capacity from the simulation to arrive at the melt constant-pressure heat capacity. The latter is in agreement with experiment. The gauche-trans ratio and the mean-square end-to-end distance are found to be independent of pressure. The latter is also found to be in agreement with the rotational isomeric state model.

It is well-known that the simulation of molecular packing in dense polymer fluids is an extraordinarily difficult problem. Yet the ability to describe in detail the packing under these circumstances is of paramount importance in the general area of structure-property prediction and correlation in polymeric materials. The difficulty in simulation lies, of course, in the molecular connectivity. In a polymer melt, the molecules are visiting conformational space by virtue of many cooperative bond rotations. The slow physical time scale of these bond rotations,  $10^{-6}$  s or longer in most applications of interest, precludes the direct attack via molecular dynamics (MD) where the basic time step is  $\sim 10^{-15}$  s. Use of Monte Carlo methods in the equilibrium situation is not straightforward because of the difficulty in finding elementary moves that lead to exploring efficiently the intramolecular conformational space under the restrictions of the intermolecular packing. Lattice methods have been extensively applied to Monte Carlo simulation of polymer fluids. Although sacrifice in physical realism is made, they are inherently faster than an unrestricted or off-lattice method. The problem of finding acceptable moves in conformational space in the presence of dense intermolecular packing is exacerbated

on the lattice. However, very significant progress has been made as the result of the realization that reptational moves provide a means of sampling conformational space that is efficient enough to allow simulation of molecules of reasonable length in dense, but not fully occupied, lattices.<sup>1-4</sup> There has been some work off-lattice. Reptational moves have been employed in a fluid of chains consisting of harmonically connected beads.<sup>5</sup> There is one study where the reptational method has been used off-lattice and a realistic torsional potential employed.<sup>6</sup> Although the results were not extensive, the method appears quite successful.

Another weakness of simulations with respect to realism is the fact that constant volume has been used. The structural or molecular packing changes in the polymeric melt with temperature could be very important in the context of vitrification and property change in general. However, the changes under constant volume simulation will be very different from the constant pressure conditions of nearly all experiments. Motivated by a desire to simulate a system realistic enough from a molecular point of view to be able to make property predictions for comparison with experiment, we have investigated here the

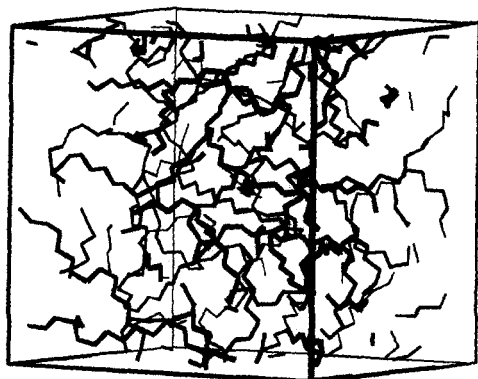


**Figure 1.** Periodic box containing 32 chains of 24 methylene units each.

feasibility of off-lattice reptational simulation under constant-pressure conditions. Formal inclusion of constant pressure in the Monte Carlo method is straightforward. However, it adds a level of uncertainty with respect to the practicality of finding acceptable moves. Volume fluctuations are to be included in the evolution of the system. The question, then, is whether in an intertwining polymeric melt volume fluctuation can be efficiently introduced. We have found in the work reported here that, although it does add to the computational time, it is possible to make this inclusion. It is thus possible to generate *PVT* and other data on a model system that is realistic enough for comparison with experiment.

### Model and Computational Details

**Molecular Model.** Polymethylene was chosen as the system to model. For computational simplicity in this feasibility study, the methylene units were represented as a single force center, and the hydrogens were not explicitly included. A nonbonded potential for interaction between such units used was previously used by us some time ago,<sup>7</sup> and it was adopted without modification. It is of the "6-12" form,

$$U(R) = 21.823 \times 10^6 / R^{12} - 6576.4 / R^6 \quad (1)$$

where energy,  $U(R)$ , is in kilojoules/mole and  $R$  in angstroms. The torsional potential

$$U(\phi) = (1/2)13.39(1 + \cos 3\phi) + (1/2)3.35(1 + \cos \phi) \quad (2)$$

was taken from the same source. It provides for a gauche-trans energy difference of 2.5 kJ/mol and a cis barrier ( $\phi = 0$ ) of 16.74 kJ/mol. The molecules were internally rigid with respect to bond stretching (bond length = 1.54 Å) and bending (valence angle = 109.47°). Nonbonded interactions were included intramolecularly only when centers were separated by four or more bonds. Thus, they do not contribute to the gauche-trans energy difference, and the latter arises solely from the torsional potential. The system consisted of a cubic box with periodic boundary conditions, and it contained 32 chains of 24 methylene units each; see Figure 1. The box size is a variable in the simulation.

**Monte Carlo Model.** The standard reptational procedure of proposing a move of a bead from one end of a chain to the other and accepting or rejecting under the Metropolis rules<sup>8</sup> was used. In addition, nonreptational torsional moves at one end only were included. After a number of reptation or purely torsional attempts, a volume fluctuation was attempted. Since the torsional angle is selected at random during reptation, the chains can access all of configuration space, and the classical isobaric iso-

thermal distribution function,

$$P(\mathbf{x}, V) = \exp[-\beta(U(\mathbf{x}, V) + pV)] / Z$$

$$Z = \int_0^\infty dV \int d\mathbf{x} \exp[-\beta(U(\mathbf{x}, V) + pV)] \quad (3)$$

where  $\beta = 1/k_B T$ , is simulated when the pressure times volume,  $pV$ , term is included along with the potential energy as a function of atomic coordinates,  $\mathbf{x}$ , for a given volume,  $U(\mathbf{x}, V)$ , in applying the Metropolis rules in accepting or rejecting a proposed move.

The complete recipe for the Monte Carlo simulation consists of the following:

- (a) Select an end at random.
- (b) Part of the time move the bead to the other end with a randomly selected torsional angle. Part of the time keep the bead at the selected end but change the torsional angle randomly.
- (c) Evaluate the energy change in (b); if  $\leq 0$ , accept; if  $> 0$ , accept with probability  $\exp[-\beta\Delta U(\mathbf{x}, V)]$  (i.e., if a random number,  $0 \rightarrow 1$ , is  $\leq \exp[-\beta\Delta U(\mathbf{x}, V)]$ , accept).
- (d) If the move (b) is not accepted, try again with a new torsional angle. Keep trying up to 4 times. If accepted or 4 tries are exhausted, start again at (a).
- (e) After  $N_{\text{rep/rot}}$  cycles starting at (a), attempt a volume variation by changing the periodic box size. Evaluate the energy change, but base acceptance or rejection on  $\Delta U(\mathbf{x}, V) + p\Delta V$ .
- (f) Start at (a) again for  $N_{\text{rep/rot}}$  more cycles.

The selection in (b) above between reptation and rotation without reptation was made randomly with probability = 0.5.

**Volume Fluctuation.** The practical success of the procedure above in achieving equilibrium in the constant-pressure simulation depends on the ability to experience a reasonable acceptance rate for the volume changes. It is not at all obvious that in the entangled melt this can be easily accomplished. However, it was found that a very simple strategy was practical. The cubic periodic box has an edge dimension,  $L$ , which for the work done here was in the vicinity of 30 Å. A proposed new periodic box dimension,  $L + \Delta L$ , was selected by choosing  $\Delta L$  at random between the limits  $\pm 0.5$  Å. Each chain was translated rigidly by an amount fixed by imposing a translation of the end of the chain that was affine with respect to  $L \rightarrow L + \Delta L$ . In the application of the translations, the periodic coordinates were first "unwrapped" to make each chain continuous, and then periodic boundary conditions were reimposed on the translated chains. The volume-adjusted system preserves the internal geometry and intramolecular energy of all the chains, but the intermolecular nonbonded energy change is evaluated.

**Computational Details.** As in all condensed phase simulations, the intermolecular nonbonded energy evaluation is the time-consuming step computationally. In the work done here, the energy change evaluation on reptation or a purely torsional move was accomplished in two steps. A preliminary, slightly approximate one was invoked to screen out obviously high-energy changes. It was followed by a more accurate one when appropriate. The preliminary screening used the common method of keeping neighbor lists. Since the energy change involves only the interactions between end beads and the medium, the lists involved only the neighbors of the end beads. A record was kept of the successful reptations of each end. If, in considering a move from a given end, the neighbor list of the end in question contained a member that had undergone two or more successful reptations, that list was discarded and a new one generated. At the proposed new

Table I  
Summary of a Typical Monte Carlo Run<sup>a</sup>

$g^2$	av dispersion					attempted moves	successful		vol fluct	
	$\langle R^2 \rangle$	$\langle L_{\text{box}} \rangle$	$\langle U_{\text{NB}} \rangle$	$\langle U_{\text{tor}} \rangle$	$\langle F_{\text{tr}} \rangle$		reptations	rotations	attempted	successful
521	283	28.64	-4.87	3.48	0.615	1 331 361	48 590	99 972	1000	149
	148	0.12	0.08	0.09	0.011					

<sup>a</sup> Temperature = 450 K, pressure = 400 atm. The run consisted of 400K cycles of selection of an end and up to 4 tries of each selection to move by reptation or by a torsional rotation without reptation. After every 400 of these cycles, a volume fluctuation attempt was made.  $g^2$  is the squared distance moved by a center bead from the beginning to the end of the run averaged over all of the chains in Å<sup>2</sup>;  $\langle R^2 \rangle$  is the mean-square end-to-end distance during the run averaged over all chains in Å<sup>2</sup>;  $\langle L_{\text{box}} \rangle$  is the average length of the edge of the periodic box in Å;  $\langle U_{\text{NB}} \rangle$  is the average nonbonded energy in kJ/mol;  $\langle U_{\text{tor}} \rangle$  is the average torsional energy in kJ/mol;  $\langle F_{\text{tr}} \rangle$  is the average fraction of trans bonds, i.e.,  $120^\circ < \phi < 240^\circ$ . The dispersions ( $= \sum \delta^2 / N_{\text{sample}}^{1/2}$ ) in these quantities are listed on the second line. Sampling for the averages was done every 400 move cycles. Moves column is the total number of moves attempted, reptation and torsional rotation without reptation; approximately half were reptation attempts and half rotation only. The number of successful reptations and rotations without reptation are listed separately. The execution time on the SDSC Cray XMP4/8 was 1108 s. About half of the computation time was associated with the reptation or rotation moves and about half with the volume fluctuations.

end, the neighbor list of the end to be attached to was used for the preliminary energy evaluation. The energy change on this basis was considered, and if  $\ln n_r + \beta \Delta U(\mathbf{x}, V)$  exceeded 0.25 (rather than 0), where  $n_r$  is a random number,  $0 \rightarrow 1$ , the move was rejected. If not, the energy change was reevaluated using newly generated neighbor lists for both positions and the standard Metropolis condition applied. It was found that new neighbor lists were essential in calculating the energy change accurately enough to avoid systematic errors. A sensitive monitor of such errors is keeping track of the energy change of the system by accumulating the accepted  $\Delta U$ s as a sum. These should approach a constant value, but systematic errors will result in a very strong drift in a long simulation run. The above strategy was accurate and saved computer time since most of the proposed moves were rejected in the first screening.

In computing the energy change in the volume fluctuation, all of the beads have to have their nonbonded energy evaluated and a fresh list was generated. It was found that the same list could be used before and after, however, if a truncation correction were made. The energy beyond the cut-off radius is evaluated from the  $R^{-6}$  attractive energy only as

$$U_{\text{trunc}} = - \left( \int_{R_{\text{max}}}^{\infty} n C R^{-6} 4\pi R^2 dR \right) = - \frac{4\pi}{3} n \frac{C}{R_{\text{max}}^3} \quad (4)$$

where  $n$  is the number density of centers,  $C$  is the coefficient in the attractive potential in eq 1, and  $R_{\text{max}}$  is the nonbonded cut-off. The total truncation correction for  $N$  atoms in a box of dimension  $L_1$  before volume fluctuation and  $L_2$  afterward is

$$\delta U_{\text{trunc}} = - \frac{1}{2} N \frac{4\pi}{3} C \left( \frac{n_2}{R_{\text{max}}^3(2)} - \frac{n_1}{R_{\text{max}}^3(1)} \right) \quad (5)$$

where  $R_{\text{max}}(2) = R_{\text{max}}(1)L_2/L_1$  and the number densities are  $n_1 = N/L_1^3$  and  $n_2 = N/L_2^3$ , and it is implied that the nonbonded list is generated for state 1 with  $R_{\text{max}}^*(1)$  and is also used for state 2. The factor of  $1/2$  in eq 5 comes from not counting the pair interactions twice.

The computations were run on the Cray XMP 4/8 at the San Diego Supercomputer Center and were coded in Cray CFT FORTRAN. In the nonbonded energies computations and in other tasks, the nearest periodic image of a given neighbor must be found. The Cray "conditional vector merge" functions were utilized in this endeavor to permit vectorization.<sup>9</sup> A value of  $R_{\text{max}} = 9.0$  Å was used in all of the computations reported here.

Originally, the simulations were started from an ordered array of planar zigzag chains in the periodic box. After this initial step, however, simulation runs under various

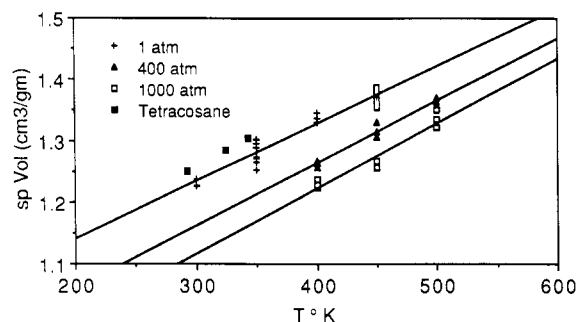


Figure 2. Specific volume versus temperature along three isobars. The points are the results of individual simulation runs such as described in Table I, except at 450 and 1 atm where the vertical dimension of the box indicates the standard deviation of 11 runs. The lines are least-squares fits. The points shown for tetracosane,  $C_{24}H_{50}$ , are experimental (1 atm), ref 10.

conditions were started from the finish of a another run, perhaps under different  $T$  and  $P$  conditions. Statistics were accumulated by sampling the system after every  $N_{\text{sample}}$  cycles through (a)–(f) above. Equilibration runs were made before runs where results were recorded. In reptation, a key issue is whether all of the bonds in a chain are being accessed in moves. A measure of this which seemed to be a good measure of equilibrium was the mean-square distance that a center bead traversed, averaged over the chains, during the run compared to the mean-square end-to-end distance, averaged over the chains. Equilibration seemed to be achieved when the former was comparable to or greater than the latter. Thus, the run lengths were tailored to achieve this. A précis of a typical run is shown in Table I.

Data were taken for runs over the temperature range 300–500 K and the pressure range 1–1000 atm. At 1 atm, difficulty was experienced in achieving the equilibrium condition with respect to center bead diffusion much below 300 K, and this difficulty increased with increasing pressure.

## Discussion of Results

**PVT Data.** In our initial runs, it became apparent that it was possible to achieve equilibrium at 1 atm with respect to volume adjustments under the method chosen. Other runs were then made over a range of pressures and temperatures. The specific volumes as a function of temperature for isobars at 1, 400, and 1000 atm are shown in Figure 2. Three experimental values are shown for the specific volume of  $C_{24}H_{50}$ , tetracosane.<sup>10</sup> They agree with the value calculated here to 2%. Along the 1-atm isobar in Figure 2, the experimental specific volume of polyethylene (PE)<sup>11</sup> itself lies ~5% below the calculated values. Since tetracosane experimentally lies above the

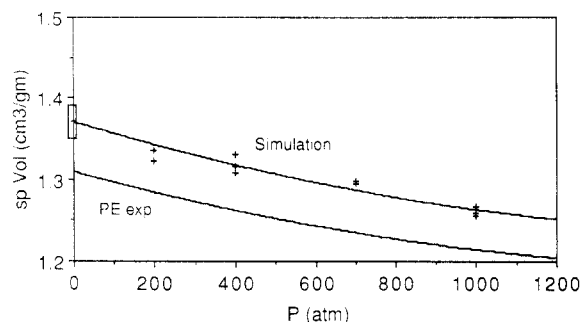


**Figure 3.** Specific volume versus pressure at 450 K. The points are individual simulation runs, except for 1 atm where the vertical dimension of the box indicates the standard deviation of 11 runs. The curves through the points is a least-squares second-order polynomial ( $V = 1.370 - (1.485 \times 10^{-4})P + (4.107 \times 10^{-8})P^2$ ). The curve without points is the experimental behavior of PE, ref 11.

calculated isobar, the lower values for PE are presumably a molecular weight effect; the  $C_{24}$  chains simulated are not long enough for the volume itself to reach the long chain value. Perhaps a better way of describing this is as an end-group effect. The terminal groups occupy more volume than the chain methylene units. However, the calculated coefficient of thermal expansion along 1 atm agrees rather well with experiment for PE,  $7.3 \times 10^{-4} \text{ } ^\circ\text{C}^{-1}$  calculated versus  $6.9 \times 10^{-4} \text{ } ^\circ\text{C}^{-1}$  at 100  $^\circ\text{C}$ , experimentally as reported by Maloney and Prausnitz.<sup>11</sup>

A calculated isotherm at 450 K is shown in Figure 3. Also shown is the experimental curve for PE at this temperature. The latter was deduced from the Tait equation reported by Maloney and Prausnitz<sup>11</sup> and used with their parameters (for  $T = 450 \text{ K}$ ) that were determined to fit PE in this region of temperature and pressure. Because of the  $\sim 5\%$  specific volume offset commented on above and ascribed to a molecular weight or end-group effect, the experimental PE curve falls below the calculated one here. However, they are parallel and show similar curvature, indicating agreement of the calculated isothermal compressibility and its dependence on pressure.

**Heat Capacity.** Since the simulation leads to realistic PVT behavior, it seemed appropriate to extract other equilibrium properties. The constant pressure heat capacity,  $C_p$ , would be especially welcome in the study of liquid polymer molecular structure. There are two reasons why this cannot be extracted directly. The model is a classical one, and the internal molecular vibrational contributions are largely still well below the classical limits. Further we excluded bond stretching and bending from the model and did not explicitly include hydrogens. However, these problems can be circumvented to a good approximation. A number of individual chains were isolated from the simulation and hydrogens added. These were then subjected to harmonic vibrational analysis with a complete force field and degrees of freedom. The vibrational thermodynamic functions were calculated and averaged for these molecules. It was found that there was little variation in the functions among the selected conformationally disordered molecules from the simulation. Two contributions were then added to these functions. The first was the heat capacity determined from the temperature dependence of the intermolecular nonbonded energy. The other was the heat capacity from the temperature dependence of the average number of gauche bonds. The latter were assigned an energy of 2.5 kJ/mol from the torsional potential, eq 2. Since the heat capacity from these two sources was determined from the temperature dependence of average energies or average fraction of gauche bonds and there was statistical scatter in

**Table II**  
Contributions to the Constant-Pressure Heat Capacity

T, K	internal vibrational	intermol	G/T population	total, J/mol/K
300	19.62	6.07	1.21	26.9
350	23.01	6.07	1.21	30.3
400	26.40	6.07	1.21	33.7
450	28.57	6.07	1.21	35.9

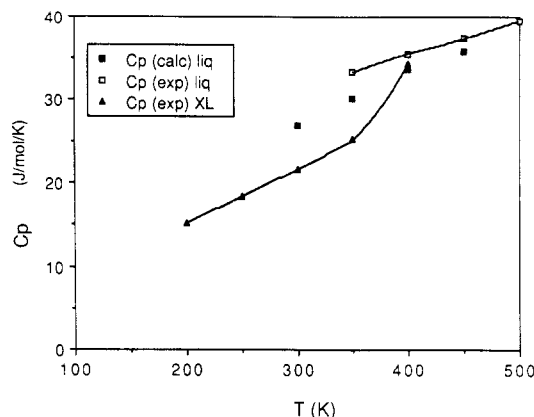


**Figure 4.** Heat capacity of the liquid from the simulations, filled squares, compared with experimental values, ref 12, for PE solid (curve through the triangles) and PE liquid (curve through the open squares).

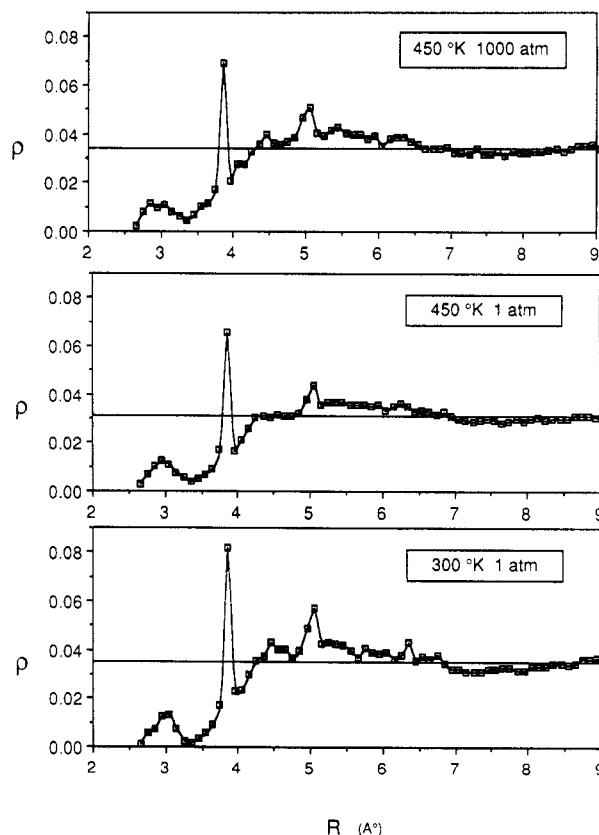


**Figure 5.** Radial distribution functions (methylenes/ $\text{\AA}^3$ ,  $\Delta r$  increment = 0.1  $\text{\AA}$ ) at the extrema of temperatures (300, 450 K) simulated at 1 atm and at 1000 atm at 450 K. Mean number densities are indicated by the horizontal lines.

the numbers, there was not sufficient discrimination to determine the temperature dependence of the heat capacities, and they were taken as a temperature-independent average over the range 300–450 K. The heat capacity contributions from all three sources are shown in Table II. A plot and comparison with experiment<sup>12</sup> are

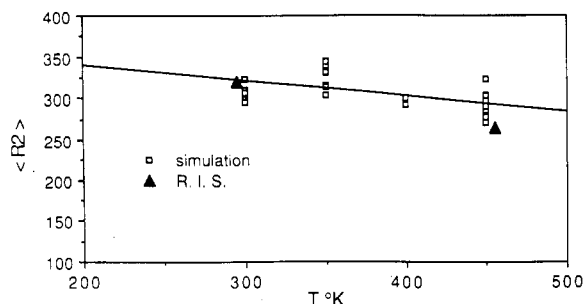


**Figure 6.** Mean-square end-to-end distance ( $\text{\AA}^2$ ) versus temperature at 1 atm. The line is a least-squares fit (slope =  $0.18 \text{ \AA}^2/\text{K}$ ). Also shown are the results of a rotational isomeric state conclusion (R.I.S.), see text for details.

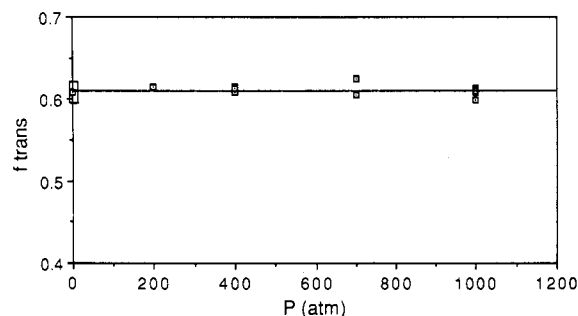


**Figure 7.** Fraction of trans bonds ( $120^\circ < \phi < 240^\circ$ ) versus pressure at 450 K. The line is a least-squares fit.

shown in Figure 4. The agreement is very reasonable.

Another way of constructing the heat capacity would have been to use the simulated torsional energy as a classical integration over the torsional space and not have included the term in the temperature dependence of the gauche energy of the bonds. This would have had the advantage of introducing torsional anharmonicity in a more rigorous way but would have required deleting the torsional modes from the harmonic analysis. In view of the complexity of this, we elected to defer investigating this option until later.

#### Effect of Temperature and Pressure on Structure.

Radial distribution functions at the limits of temperatures simulated at 1 atm (300, 450 K) and at 1000 atm (450 K) are shown in Figure 5. The effect of temperature on the gauche-trans ratio may be seen in the peaks at  $\sim 3.0$  and  $3.9 \text{ \AA}$ . The effect of temperature at 1 atm on the mean-square end-to-end distance is shown in Figure 6.

It is by now widely appreciated that the melt should be a similar to a  $\Theta$  solvent and that a comparison with the average dimensions deduced from the rotational isomeric state theory<sup>14</sup> is an appropriate undertaking. It is not possible to make a precise comparison because the model here samples all torsional space rather than discrete values. However, the values of  $E_g$  (the gauche-trans energy difference) =  $2510 \text{ J/mol}$  ( $600 \text{ cal/mol}$ ),  $E_w$  (the "pentane interference" energy) =  $6276 \text{ J/mol}$  ( $1500 \text{ cal/mol}$ ),  $\phi_g = 65^\circ$  along with the bond length, and valence angle of the model would seem to be suitable for the model here. When entered in the formalism of the finite-chain characteristic ratio calculation,<sup>14</sup> they lead for a  $C_{24}$  chain to the values shown in Figure 6. Although the scatter in the simulation results is considerable, the agreement is satisfactory, a

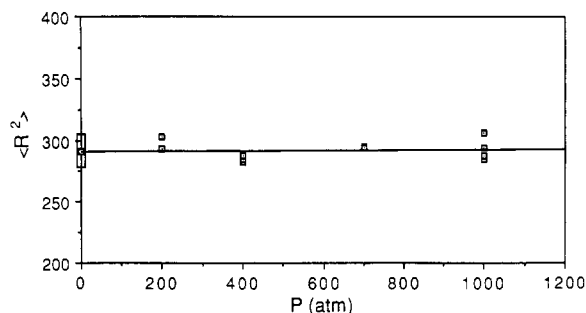


**Figure 8.** Mean-square end-to-end distance versus pressure at 450 K. The line is a least-squares fit.

conclusion reached previously.<sup>6</sup>

The effect of pressure on the intramolecular conformational makeup is of interest of the context of experiments and simulations on *n*-butane<sup>13</sup> and also the question of  $\Theta$  conditions obtained in melts.<sup>14</sup> As seen in Figure 7, no observable effect of pressure on the gauche-trans ratio was found. In addition, the mean-square end-to-end distance was found to be independent of pressure, Figure 8. It would appear that at the chain lengths studied here there is no efficiency of packing resulting from favoring trans or gauche conformations promoted by densification at pressures up to 1000 atm.

**Acknowledgment.** The author is indebted to the US Army Research Office for financial support of the portions of this work dealing with methods for generating realistically disordered polymer structures and to the Polymers Program, Division of Materials Research, National Science Foundation for the portions dealing with the structure and properties of polymeric liquids. The author is also indebted to the National Science Foundation supported San Diego Supercomputer Center for a grant of computer time. He thanks Prof. W. L. Jorgensen for a helpful discussion and Grant D. Smith for carrying out the R. I. S. calculation.

**Registry No.** PE, 9002-88-4;  $C_{24}H_{50}$ , 646-31-1; polymethylene, 25038-57-7.

#### References and Notes

- (1) Baumgaertner, A. *J. Chem. Phys.* **1986**, *84*, 1905. A number of references to previous work are contained here also.
- (2) Kolinski, A.; Skolnick, J.; Yaris, R. *Macromolecules* **1986**, *19*, 2550, 2560.
- (3) Kolinski, A.; Skolnick, J.; Yaris, R. *J. Chem. Phys.* **1987**, *86*, 1567, 7164.
- (4) Kremer, K. *Macromolecules* **1983**, *16*, 1632.
- (5) Bishop, M.; Ceperly, D.; Frisch, H. L.; Kalos, M. H. *J. Chem. Phys.* **1980**, *72*, 3228.
- (6) Vacatello, M.; Avitabile, G.; Corradini, P.; Tuzi, A. *J. Chem. Phys.* **1980**, *73*, 548.
- (7) Boyd, R. H.; Breitling, S. M. *Macromolecules* **1974**, *7*, 855.
- (8) Metropolis, N.; Rosenbluth, A. N.; Rosenbluth, M. N.; Teller, A. H.; Teller, E. *J. Chem. Phys.* **1953**, *21*, 1087.
- (9) van Gunsteren, W. F.; Berendsen, H. J. C.; Colonna, F.; Perahia, D.; Hollenberg, J. P.; Lellouch, D. *J. Comput. Chem.* **1984**, *5*, 272.
- (10) *Handbook of Chemistry and Physics*; Weast, R. C., Ed.; Chemical Rubber: Cleveland, 1969, 50th ed.; 1949, 31st ed.
- (11) Maloney, D. P.; Prausnitz, J. M. *J. Polym. Sci., Polym. Phys. Ed.* **1974**, *18*, 2703.
- (12) Gaur, U.; Wunderlich, B. *J. Phys. Chem. Ref. Data* **1981**, *10*, 119.
- (13) Jorgensen, W. L. *J. Phys. Chem.* **1983**, *87*, 5304.
- (14) Flory, P. J. *Statistical Mechanics of Chain Molecules*; Interscience: New York, 1967.